Experimental Investigation of the Unsteady Flow Behavior on a Film Cooling Flat plate

S.Rouina[a] , M.Miranda[a],G.Barigozzi[a],*

aDipartimento di Ingegneria-Università di Bergamo, Viale Marconi 5, 24044 Dalmine, BG, Italy

Abstract

An experimental study was conducted to investigate the unsteady behavior of film cooling for cylindrical holes on a flat plate wind tunnel. Tests have been carried out at low speed and low inlet turbulence intensity level, with blowing ratios varied in the range 0.5–1.5. Aerodynamic investigations have been performed through the measurement of discharge coefficients in order to characterize the blowing conditions. A Laser Doppler Velocimetry (LDV) was then used to study the boundary layer behavior just downstream of the holes for variable injection condition. A high resolution PIV system was finally used for flow visualization and flow field measurement to investigate the unsteady mixing process taking place between coolant and main flow. For low blowing ratios, the jet stays close to the surface; traces of coherent vortical structures are detected only far from injection, which appear as clockwise vortices. Increasing the blowing ratio leads to the appearance of counter-clockwise vortical structures due to the breakdown of the Kelvin Helmholtz instability of the shear layers.

Keywords:

1. Introduction

As well known, turbine inlet temperature is the driving parameter to improve gas turbine performance. Hot components in modern gas turbine engines work at temperature levels well above the limit imposed by technological constrains. As a result, efficient cooling system is required to ensure that turbine vanes and blades withstand such

---

* Corresponding author. Tel.: +39 035 2052317; fax: +39 035 2052077.
  E-mail address: giovanna.barigozzi@unibg.it

high thermal loads. In modern gas turbine, film cooling is extensively used, together with internal cooling, to cool all the exposed surfaces, i.e. vanes, rotor blades and platform. Film cooling not only determines the heat exchange characteristics of the airfoils, but also affects its aerodynamic performance. The main effects are on the one hand a reduction of the adiabatic wall temperature and on the other the aerodynamic mixing between main and coolant flow, which results in a general increase of losses with a consequent decrease in the aerodynamic efficiency of the component. The injection of a jet in a main flow in fact implies the establishment of a three-dimensional flow, in which counter-rotating vortices, the so called kidney vortex pair, appear [1]. These vortices are responsible for the entrainment of hot main flow towards the wall, resulting in a decrease of thermal protection. So, accurate information on the interaction of coolant injection with boundary layers developing on the airfoils is required to optimize the cooling design from the aerodynamic and thermal point of view.

Nomenclature

BR	blowing rate
C_d	discharge coefficient
D	diameter
H_{12}	shape factor
L	axial length
P	span-wise pitch
P	pressure
Tu	turbulence intensity, %
U	stream-wise velocity
u',v'	stream-wise and pitch-wise RMS velocity components
X, Y, Z	Cartesian coordinate system
δ	boundary layer thickness
δ^*	displacement thickness

Subscript

c	cooling flow
∞	Freestream

Vast numbers of investigation have been carried out considering the influence of various parameters, e.g., hole geometry, blowing, momentum and density ratio and free-stream turbulence on coolant interaction with the mainstream [1,2]. The geometry of the film cooling hole has a profound impact on the coverage of the film. Film cooling holes with low injection angles provide a better coverage in the downstream region when compared with 90° injection, since coolant remains attached to the surface over a greater distance. The same beneficial effect can be obtained by shaping the hole exit section. Adding a diffusion section at the hole exit in fact reduces the jet momentum, allowing it to stay closer to the wall, in the meanwhile distributing the coolant over a wider region. In addition, the amount of coolant flowing through the hole (and thus the blowing ratio BR) affects how the coolant interacts with the mainstream, and therefore, optimizing the blowing ratio is critical because blowing rates that are too high lose more coolant into the mainstream, whereas low blowing ratios do not provide enough coolant to effectively cover the surface. For simple cylindrical holes, it has been shown that the optimum blowing ratio is approximately BR=0.5–0.8 [3-5].

Most of data available in the literature refer to averaged information, i.e. assume that the jet to mainstream mixing process can be considered as a steady problem. Recent studies have shown that jet to mainstream mixing process is in fact an unsteady and highly anisotropic phenomenon [6]. Different coherent structures were observed at the jet boundaries, depending on the jet to mainstream velocity ratio. Coherent unsteadiness consisting in Kelvin–Helmholtz vortices were observed for high blowing ratios while hairpin vortices appeared at lower blowing ratio.

Several CFD studies on film cooling are also available in the published journals. Most of them have been done using steady Reynolds-averaged Navier-Stokes (RANS) calculation procedures. Harrison and Bogard [7] have examined the effects of various turbulence models by comparing laterally averaged, centerline, and lateral

distributions for both adiabatic effectiveness and heat transfer coefficient augmentation. All turbulence models provide poor predictions of lateral distributions due to lack of sufficient lateral spreading. Although anisotropic use of the RSM (Reynold's stress) model, simulations did not result in significantly better lateral spreading.

Much better prediction capability can be obtained by using simulation approaches like DES or LES. Foroutan and Yavuzkurt [8] investigate the flow field and heat transfer in film cooling with a single-row of cylindrical holes on a flat plate applying RANS and hybrid URANS/LES models. It is shown that hybrid URANS/LES models predict more mixing both in the wall-normal and span-wise directions compared to RANS models, while unsteady asymmetric vortical structures of the flow can also be captured. The turbulent heat flux components predicted by the DES model are higher than those obtained by the RANS simulations, resulting in enhanced turbulent heat transfer between the jet and mainstream, and consequently better predictions of the effectiveness. The unsteady CFD approach in turns requires detailed experimental data to be fully validated. In recent year, some attempts have been done to study unsteady jet to mainstream interaction in the near hole exit region using PIV system. Barigozzi et al. [9] investigated the unsteady behavior of cooling jet on a pressure side vane surface and on a cutback trailing edge, using PIV flow visualization. Furthermore, Wright et al. [10] investigated the effect of freestream turbulence intensity on film cooling jet structure using PIV flow field measurements. All these studies demonstrate that PIV has the potential to capture the unsteady behavior of film cooling jet effectively.

The present paper is aimed at collecting a useful data base for unsteady as well as advanced hybrid URANS-LES CFD simulations by using a simple geometry and the capability of PIV system. Experiments were conducted in a flat plate wind tunnel with cylindrical 30 degree angle holes. Tests have been carried out at low speed and low inlet turbulence intensity level, with blowing ratios varied in the range 0.5–1.5. Boundary layer measurements approaching the holes as well as just downstream of the holes and high speed flow visualizations were performed to fully describe, from both a time-mean and an unsteady point of view, the complex coolant-to-mainstream mixing process for variable injection conditions.

2. Experimental apparatus and testing conditions

Tests were performed in the low speed flat plate wind tunnel available at the Turbomachinery Laboratory of Bergamo University. It is a continuous running suction type wind tunnel (Fig.1a). The air is driven inside of the tunnel through an accelerating inlet section by means of a centrifugal fan. The tunnel cross section is 0.2 x 0.2 m^2, and it is 1.6 m long. The walls of the test section are optically transparent. Tests have been carried out at low speed, about 17 m/s, and low inlet turbulence intensity level. Pressure taps on the side wall (± 1 Pa) allow for a continuous monitoring of tunnel operating conditions. A diagram of the flat test plate can be seen in Fig. 1b. A row of three 5 mm diameter cylindrical holes are manufactured on the bottom wind tunnel wall. Holes have sharp edges without any fillet and are angled at 30° to the wall; their pitch-to-diameter ratio is $P/D = 6$ and their length to diameter ratio is $L/D = 10.7$. A modular manufacturing of the flat plate allows easily changing the cooling geometry. A secondary air supply system feed the coolant to the holes through a plenum. The plenum (Fig. 1c) is located beneath the wind tunnel bottom wall and consists in a box of 0.2 m x 0.11 m x 0.2 m: the air coming from the compressed air supply system enters the plenum from a 15 mm diameter side hole. Coolant injection conditions are controlled measuring the injected flow rate and pressure (± 24 Pa) and temperature inside the plenum. The injected flow rate is measured with a rotameter (± 2 l/min), while temperature is measured with a T-type thermocouple (±0.5°C).

3. Measurement techniques

A 2D component Laser Doppler Velocimetry (LDV) was used to study the boundary layer upstream ($X/D = -7$ from hole downstream edge) and just downstream of the holes ($X/D = 1$ and 5) for variable injection condition. In all cases, the measurement volume was located at mid hole centerline ($Z/D = 0$). The light source was a 300mW Ar+ laser. A 200 mm focal length front lens allowed to get a measurement volume 0.06 mm in diameter and 0.6 mm in length. Two Burst Spectrum Analyzers (DANTEC BSA) were used to process the signals coming from the photomultipliers. All measurements were carried out acquiring 20,000 burst signals at each location.

Two sets of experiments have been done by means of 2D-PIV system: flow visualizations and flow field measurements. Flow visualizations and flow field measurements were performed on stream wise plane located at the

mid hole centerline (*Z/D* = 0). Also, flow visualization were conducted from the top of wind tunnel (*Y/D* = 0.5). Illumination was provided by a double pulsed Nd: YAG laser emitting two pulses of 200 mJ at the wavelength of 532 nm with a repetition rate of 10 Hz. A CCD camera with a resolution of 2048 x 2048 pixels equipped with Nikkor lenses was used to capture images. The CCD camera and the double-pulsed Nd:YAG lasers were connected to a workstation (host computer) via a timer box which controlled the timing of the laser illumination and the image acquisition. Moreover, the data captured by the CCD camera was post-processed using Dantec software. Flow field measurements have been conducted in three steps: calibration, measurement, and analysis. A checkerboard target with spacing of 5mm x 5 mm was used to perform calibration. For each blowing ratio, 200 image pairs were recorded, and each pair of images post processed using Adaptive PIV with minimum interrogation area of 32×32 pixels and 50% overlap.

For flow field visualization only the coolant flow was seeded by means of a Laskin seeding generator making use of vegetable oil. On the other hand, for velocity flow field measurements (LDV and PIV) also mainstream was seeded by SAFEX fog generator.
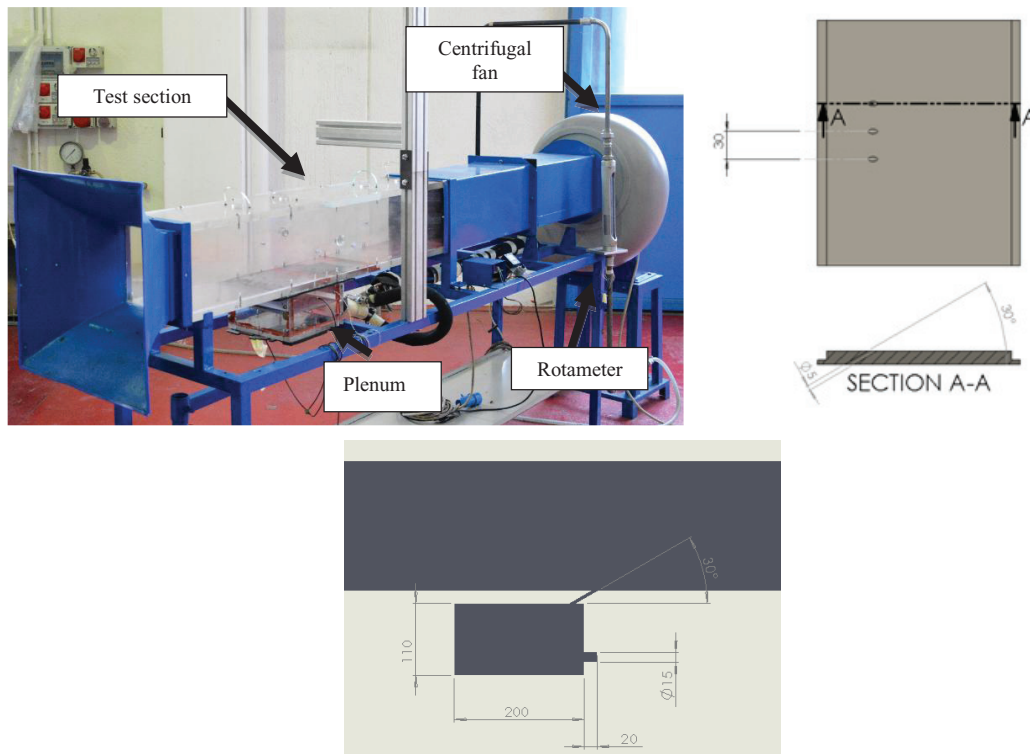

Fig. 1. (a) View of flat plate wind tunnel and (b) Schematic of flat plate and cylindrical holes (c) schematic of plenum

4. Results

Before discussing the results, the characterization of the approaching boundary layer and of the injection system will be presented. Then, boundary layer profile at different *X/D* obtained from LDV measurements will be presented for variable injection conditions. Finally, PIV flow field measurement and flow visualization for different blowing ratio will describe the coolant-to-mainstream mixing process and demonstrate the effect of different blowing ratios on film cooling jet structure.

4.1. Wind tunnel and cooling hole characterization

The approaching boundary layer was characterized by the LDV system $7D$ upstream of injection location (the origin of hole coordinate system coincides with the hole trailing edge). Fig. 2 shows the boundary layer profile as well as turbulence intensity. The measured boundary layer profile compares well with the typical 1/7 power law, also shown in Fig. 2a. The boundary layer thickness is $1.24D$, while its displacement thickness and shape factor are respectively $0.142D$ and 1.37, indicating a fully turbulent boundary layer. A free stream turbulence intensity of about 0.6% was also detected.

Hole injection characteristic was then investigated through the measurement of discharge coefficient. Fig. 2b shows the C_d distribution versus the ratio of coolant pressure $p_{t,c}$ to the free stream static pressure p_e, measured by means of pressure taps on the wind tunnel side-wall. The discharge coefficient shows the typical behavior for cylindrical holes, reaching an almost constant value of about 0.65 for pressure ratios larger than 1.004.
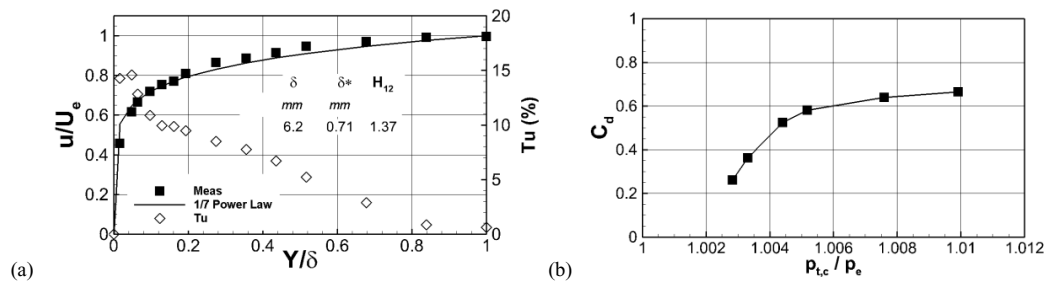

Fig. 2. (a) approaching boundary layer profile (X/D=-7) and (b) Hole discharge coefficient.

4.2. Boundary layer behavior downstream of the holes

Results from LDV measurements at hole centreline are reported in Fig.3 and Fig. 4 in terms of profiles of time averaged streamwise velocity component and streamwise and wall normal rms velocities at $X/D = 1$ and $X/D = 5$, respectively. Data are normalized with respect to the mainstream velocity U_e.

For blowing ratio less than 1, the velocity profile in Fig. 3a shows that the film cooling jet stays close to the flat plate surface with velocity always lower than the free stream one. These low velocities, associated with low fluctuations (Fig.3b-c) indicate a moderate mixing between coolant and main stream flows. On the other hand, when the blowing ratio becomes larger than 1, the streamwise velocity profile is characterized by a profound peak that becomes even higher than $1.5U_e$ for the maximum $BR = 1.5$. The elevation of this peak grows increasing the blowing ratio. Figures 3b,c depict high velocity fluctuations, especially at the jet to mainstream interfaces, and a certain degree of anisotropy, especially for the maximum $BR = 1.5$. These three figures give rise to the strong mixing between coolant and main flow with a consequent fast jet spreading in the wall-normal direction.

Comparing Fig. 3a and Fig. 4a the following can be noted: the streamwise velocity peak value decreases as the coolant travels along the flat plate surface from 1 to 5 diameters downstream of the hole due to the mixing with the mainstream. As a result, jet is spreading over a larger area. Large values for both fluctuating velocity components can still be observed $5D$ downstream of injection location, but at a higher elevation from the wall and with a more uniform distribution across the jet.

4.3. PIV Measurement Result

Figures 5 and 6 show the velocity profile in the (X,Y) plane located at the centerline of the middle hole for blowing ratio 0.75 and 1.2 respectively. It was not possible to obtain useful data for BR below 0.5, due to the laser reflection on the flat plate surface, since the jet is confined to the wall. Figure 5 depicts the normalized velocity profile for $BR = 0.75$ ($Z/D = 0$) which shows a quite uniform velocity profile which makes it difficult to distinguish

the interaction between coolant and mainstream. When increasing the *BR* to 1.2, as shown in Fig. 6, jet lifts off the flat plate surface. Also, a remarkable over speed is observed in the center of the jet which is in agreement with LDV result. These data have to be considered as preliminary results, as getting a uniform seeding distribution in the mainstream and reducing light reflections at the wall are still open issues. Nevertheless, PIV was able to capture most of the flow features, making this technique a powerful and promising instrument for film cooling unsteady characterization.
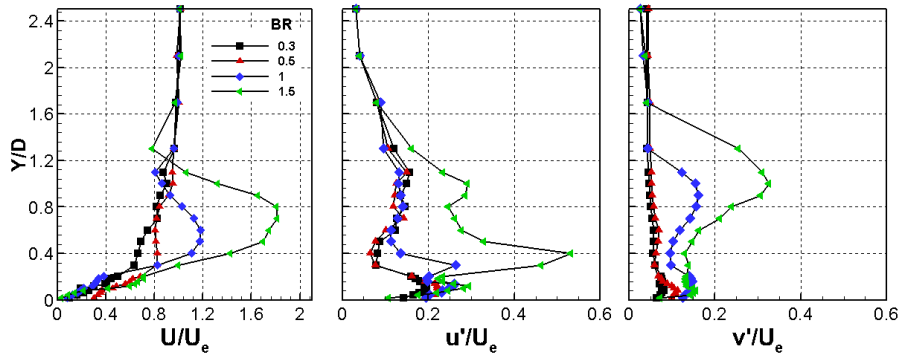
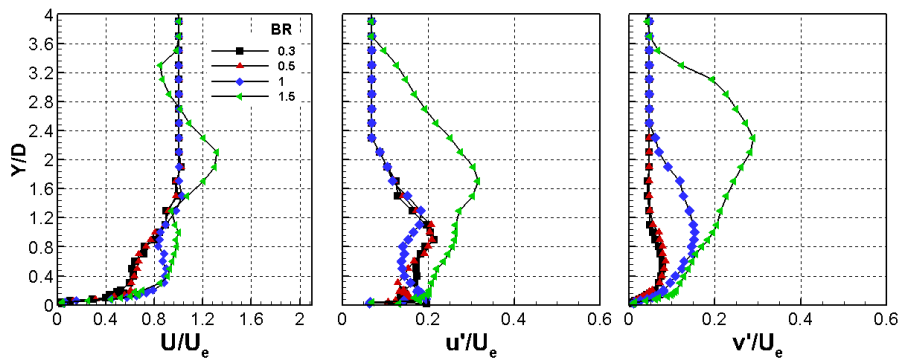

Fig. 3. Boundary layer profiles at *X/D* = 1 (*Z/D* = 0).

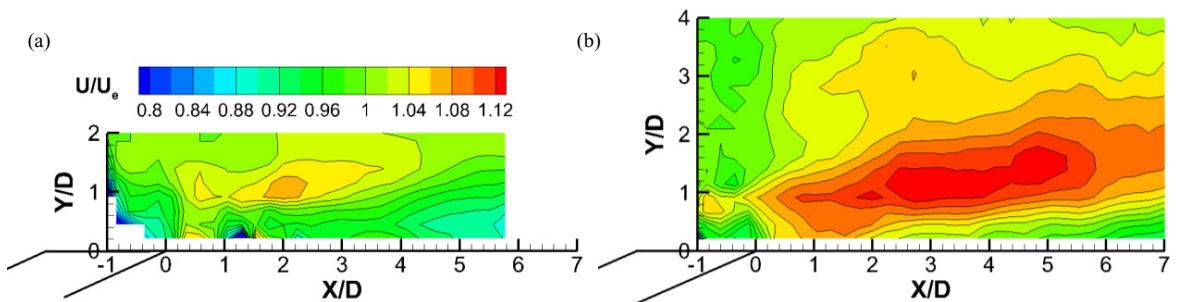
Fig. 4. Boundary layer profiles at *X/D* = 5 (*Z/D* = 0).

Fig. 5. Flow Velocity at *Z/D* = 0: (a) *BR* = 0.75; (b) *BR* = 1.2.

4.4. Flow visualization

Figure 6 reports the flow visualizations for variable injection conditions. In particular, Fig. 6a shows the coolant jet at the lowest blowing ratio tested of $BR = 0.5$. Along the centreline of the jet ($Z/D = 0$), the coolant flow remains attached to the surface downstream of the film cooling hole. 9 diameters downstream of the film cooling hole, the vertical spread of the jet is limited to 1 diameter in the vertical direction ($Y/D = 1$). Counter-clockwise vortical structures due to the breakdown of the Kelvin Helmholtz instability of the shear layers already appears at this low injection condition relatively far from the hole. This injection condition is higher than the one at which hairpin vortices were observed on a film cooled vane [9], but it is similar to the one at which counter-clockwise vortices were observed.
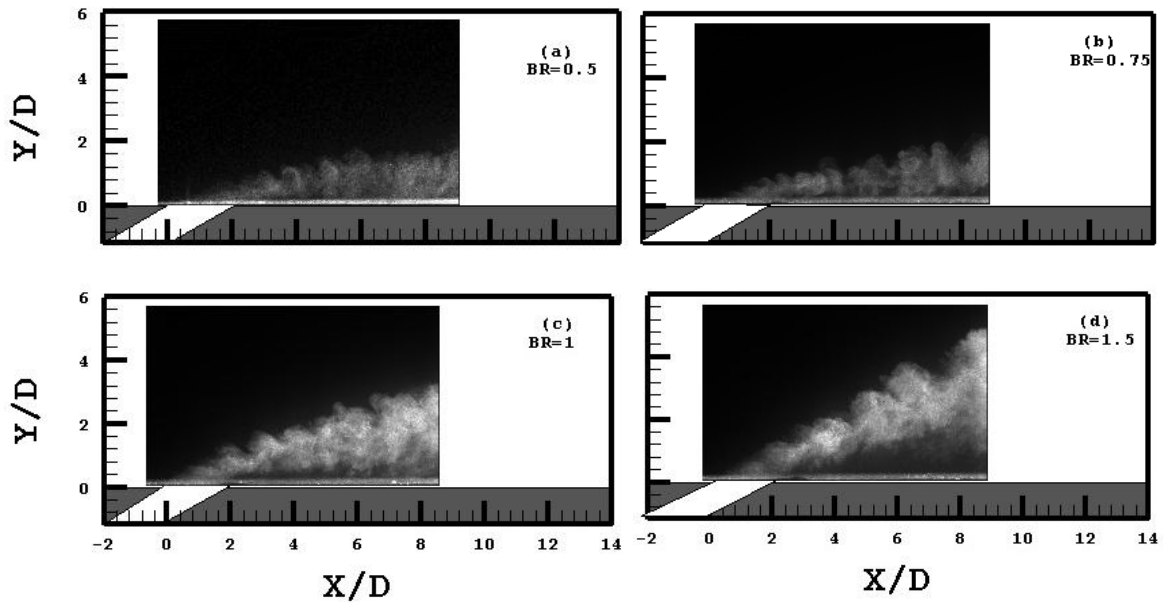

Fig. 6. Flow Visualization of film cooling jet (hole centreline): (a) BR = 0.5; (b) BR = 0.75, (c) BR = 1.0, (d) BR = 1.5.

By increasing the blowing ratio to 0.75 (Fig. 6b), these structures appears closer to injection location and result to be better defined. Film cooling jet is still attached to the flat plate surface but the vertical spread of the jet is higher than at $BR = 0.5$. Figures 6c,d demonstrate cases in which blowing ratio is larger than 1. Cooling jet begins to lift off the surface. For blowing ratio 1.5 the vertical spread of the jet has a height of $6D$ with respect to the flat plate surface which give rise to the loss of thermal protection on the flat plate surface. Moreover counter-clockwise vortical structures dominate the jet behaviour, that always result to be highly unsteady.

Figures 7a,b finally show flow visualization of film cooling jet on the flat plate surface capturing the behaviour of the cooling jet leaving three holes for $BR = 1$ and 1.5. It is not possible to capture images for blowing ratio less than 1 since the cooling film jet is attached to the surface and jet spreading in the wall-normal direction is not large enough to allow a clear jet detection. Comparison of Fig 7a with Fig 7b makes it clear that by increasing the blowing ratio jet spread over a larger area even in the lateral direction. Nevertheless, jets do not merge in the investigated domain. The coherent structures can also be observed from this point of view.
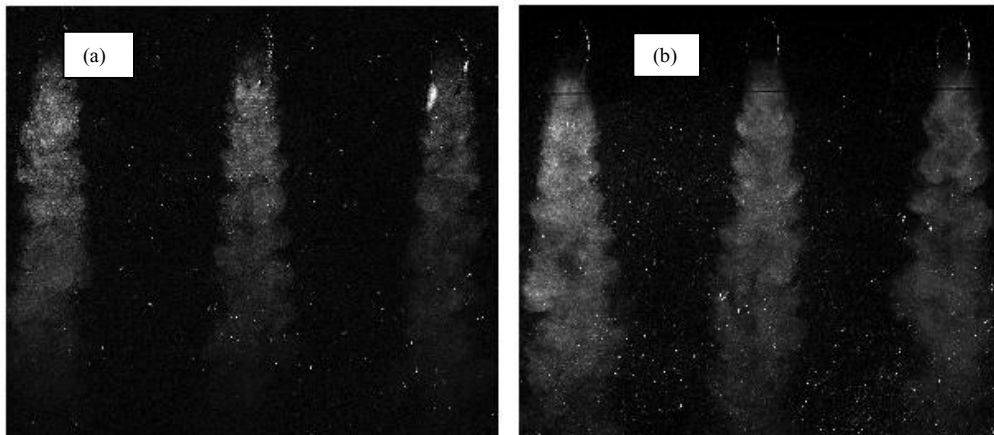
Fig. 7. Flow Visualization of film cooling jet on flat plate surface: (a) BR = 1.0; (b) BR = 1.5.

5. Conclusions

A detailed characterization of a flat plate with three cylindrical holes was carried out at low freestream turbulence intensity by varying the coolant blowing ratio from 0.3 to 1.5. Using a 2-D PIV technique which gives the opportunity to investigate the unsteady behavior of film cooling jet near the hole exit region. Flow visualizations confirmed the presence of counter clockwise rotating shear layer vortices, whatever the injection condition. In addition, PIV flow field measurements were conducted for *BR* around 1.0, and the obtained results show a good agreement with LDV data. The collected data will constitute a useful data base for unsteady as well as advanced hybrid URANS-LES CFD simulations, since the unsteady CFD approach requires detailed experimental data to be fully validated.

Acknowledgements

References

[1] Han, J. C., Dutta, S., 2000, Gas Turbine Heat Transfer and Cooling Technology, Taylor & Francis, New York, pp. 540-599.
[2] Bogard, D. G., and Thole, K. A., 2006, Gas Turbin Film Cooling, J. Propul. Power, 22, pp. 249-270.
[3] Goldstein, R. J., Eckert, E. G., and Burggraf, R., 1974, Effects of Hole Geometry and Density on Three Dimensional Film-cooling, Int. J. Heat Mass Transfer, 17, pp. 595-607.
[4] Goldstein, R. J., Eckert, E. G., Eriksen, V. L., and Ramsey, J. W., 1970, Film-Cooling Following Injection Through Inclined Circular Tubes, Isr. J. Technol., 8, pp.145-154.
[5] Jubran, B., and Brown, A., 1985, Film Cooling From Two Rows of Holes Inclined in the Streamwise and Spanwise Directions, ASME J. Eng. Gas Turbines Power, 107, pp. 84-91.
[6] Fawcett, R.J., Wheeler, A.P.S., He, L., Taylor, R. 2010, Experimental Investigation into Unsteady Effects on Film Cooling, In Proceedings of the ASME Turbo Expo, Glasgow, GT2010-22603.
[7] Harrison, K. L., Bogard, D. G., 2008, Comparison of RANS Turbulence Models For Prediction of Film Cooling Performance, In Proceedings of the ASME Turbo Expo, Berlin, GT2008-51423.
[8] Foroutan, H., Yavuzkurt, S., 2015, Numerical Simulation of the Near-Field Region of Film Cooling Jets Under High Free Stream Turbulence: Application of RANS and Hybrid URANS/Large Eddy Simulation Models, Journal of Heat Transfer 137(1) 011701.
[9] Barigozzi, G., Ravelli, S., Armellini, A., Mucignat, C., Casarsa, L., 2013, Effects of Injection Conditions and Mach Number on Unsteadiness Arising Within Coolant Jets Over a Pressure Side Vane Surface, Int. J. of Heat and Mass Transfer 67, p 1220–1230.
[10] Wright, L., M., McClain, S., T., Clemenson, M., D., 2011, Effect of Free stream Turbulence Intensity on Film Cooling Jet Structure and Surface Effectiveness Using PIV and PSP, J. of Turbomachinery, Vol 133,041023.